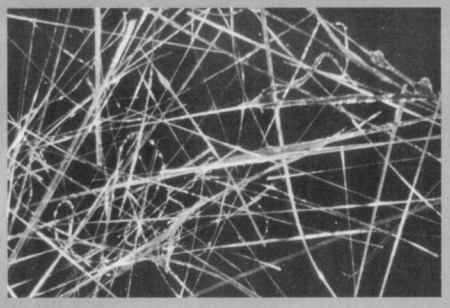

Hawaiian and Strombolian Eruptions

S. Vergniolle
The Australian National University and Institut de Physique du Globe de Paris

M. Mangan
U.S. Geological Survey

Glossary

annular flow Two-phase flow (gas and liquid) in a tube. Central gas jet surrounded by an annulus of magma. Volcanic equivalent: hawaiian fire fountains.

gas–piston activity A rhythmic rise and fall of the magma level within a volcanic conduit due to ascent and escape of large pockets of magmatic gas.

Hawaiian eruptions Basaltic eruptions with very low viscosity magma (10–100 Pa s). Fire fountains and lava flows. Examples: Kilauea Iki (United States), Piton de la Fournaise (France), Heimaey (1973, Iceland).

lava fountain A pillar-like jet of gas and molten pyroclasts that towers tens to hundreds of meters above a central vent.

lava pond An accumulation of coalesced molten pyroclasts that are trapped at the vent by the walls of a developing spatter or cinder cone.

pyroclast A general term for any fragment of lava ejected during an explosive volcanic eruption.

reticulite A delicate scoria containing 95–99% void space within a honeycomb-like network of thin glass struts.

scoria A porous, glassy pyroclast containing 70–85% void space.

slug flow Two-phase flow (gas and liquid) in a tube. Large gas pocket rising in a liquid and filling up the entire width of the conduit. Characteristic of strombolian explosions and gas–piston events during hawaiian eruptions.

spatter bombs A glassy pyroclast >64 mm across that develops a fluidal shape by the force of ejection.

Strombolian eruptions Basaltic eruptions with a low viscosity magma (100–1000 Pa s). Series of explosions. Examples: Pacaya (Guatemala), Paricutin (Mexico), Sakurajima (Japan), Stromboli (Italy), Tolbachik (Russia), Yasur (Vanuatu).

tremor A continuous vibration of the ground around active volcanoes.

HAWAIIAN AND STROMBOLIAN eruptions are the least violent, and perhaps the most majestic, form of volcanism. Their subdued intensity, magnitude, and dispersive power are the consequence of the low viscosity of the magma erupted, typically basalt or basaltic andesite, which allows gas to segregate and escape with relative ease. During strombolian eruptions,

gas is released in discrete, often rhythmic, bursts, each of which disrupts the top of the magma column and ejects a shower of incandescent lava fragments, or pyroclasts (e.g., long-standing eruptions of Stromboli, Aeolian Islands or Mount Etna, Sicily; 1943–1954 Paricutin, Mexico; 1993–1995 Mount Veniaminof, Alaska; 1995–1996 Pacaya, Guatamala; 1996 Rabaul, Papua New Guinea; 1996–1998 Villarrica, Chile). During hawaiian eruptions, gas is also released in discrete rhythmic bursts and each burst in gas flux gives rise to a sustained lava fountain (e.g., 1959, 1969, 1983–1986 Kilauea and 1950, 1975, 1984 Mauna Loa eruptions in Hawaii; 1992, 1998 Piton de la Fournaise, Reunion Island).

In actuality, a continuum exists between the two styles of volcanism, and it is not uncommon for one type of activity to give way to the other (e.g., 1961 Askja and 1973 Heimaey, Iceland; 1975 Tolbachik, Kamchatka; 1987 Izu-Oshima, Japan; 1996 Mount Etna, Sicily; 1996–1997 Pavlof and 1997 Okmok, Aleutian Islands). In this chapter, we first describe the end member characteristics of strombolian and hawaiian eruptions and then integrate these observations with two-phase flow models (e.g., analog gas–liquid systems) to infer the dynamics of hawaiian and strombolian eruptions and the transition between them.

1. DEFINING CHARACTERISTICS

A. Eruptive Style

Hawaiian-style eruptions begin with a swarm of propagating earthquakes and ground fissures. Vents spawn along a fissure as it lengthens, creating a wall of lava, or "curtain of fire," that may extend for kilometers (Fig. 1A; see also color insert). Gradually, over a period of hours to days, differential cooling due to irregularities in the width of the feeder dike causes wall solidification at narrow points. Parts of the fissure seal off, and the original line-source (Fig. 1A) becomes a point-source (Fig. 1B). The curtain of fire collapses back into a single, pillar-like fountain towering above a central vent (Fig. 1B). During a fountaining episode, the vent expels approximately 50–1000 $m^3\ s^{-1}$ of lava, which rises to heights h of 100–500 m and occasionally higher. Unusually high fountains reaching upward of 1600 m were observed during the 1986–1987 eruption of Izu-Oshima volcano (Japan).

The structure of the fountain is essentially that of a sustained gas jet carrying a dispersed load of centimeter- to meter-sized, molten clots. Gas emission and lava volume measurements made during the 1983–1986 eruption of Kilauea volcano give average effusion rates of 4.7×10^5 kg s^{-1} lava (dense rock equivalent) and 2.5 10^3 kg s^{-1} gas (0.42 wt% combined H_2O, CO_2, SO_2). The gas to clot ratio averaged for the eruption is 70 : 1 by volume, assuming lava and gas densities of 2700 and 0.2 kg m^{-3}, respectively. The clots exit at near vertical angles at speeds v, determined from the ballistic approximation $v^2 = 2gh$, of $\approx$ 100 m s^{-1}. Eruption temperatures are highest in the center of the fountain, creating an incandescent yellow-white axis that extends almost to the top of the fountain. Eruption temperatures ranging between 1150°C (1986–1987 Izu-Oshima eruption) and 1216°C (1959 Kilauea eruption) have been reported. The hot, thermal core of the fountain passes outward into a fiery orange-red region of slightly cooler temperature and lower clot density, and then to a sparse, black halo of chilled pyroclasts. Although the jetting is continuous, brightly glowing fronts pulse upward through the core of the fountain at 1- to 5-s intervals.

A central vent (i.e., a point source, Fig. 1B) may experience many fountaining episodes. The 4-week-long eruption of Kilauea volcano in 1959, for example, underwent 16 2- to 32-hour fountaining phases after the initial outburst. Typically, the fountaining ends with magma draining to deep levels in conduit amid sporadic bursts of molten ejecta and gas, and then gradually, over periods of several hours to days, it rises in preparation for the next event. As it nears the surface, the level of magma in the conduit may begin to rise and fall rhythmically (gas–piston activity) due to the ascension and release of large gas pockets (e.g., 1969–1971 and 1983–1986 eruptions of Kilauea; Fig. 2). The top of the column begins to churn and a low, commonly dome-shaped, lava fountain spawns as the new episode commences. Usually within several tens of minutes to a few hours the incipient fountain builds to a maximum height, which may hold constant through a significant part of the episode. The end of each episode is often abrupt compared to the period of buildup. In the first 17 fountaining cycles of the 1983–1986 eruption of Kilauea volcano, for example, 100- to 300-m fountains built up over several tens of minutes to 2 hours time, whereas the height usually dropped to zero in 3–10 minutes at the end of the episode.

It is not unusual for a long span of successive fountaining episodes to yield to an era of continuous, quiescent lava effusion before the eruption finally comes to an end (e.g., the 1969–1971 and 1983 to present eruptions of Kilauea). The long-standing eruption of Kilauea vol-

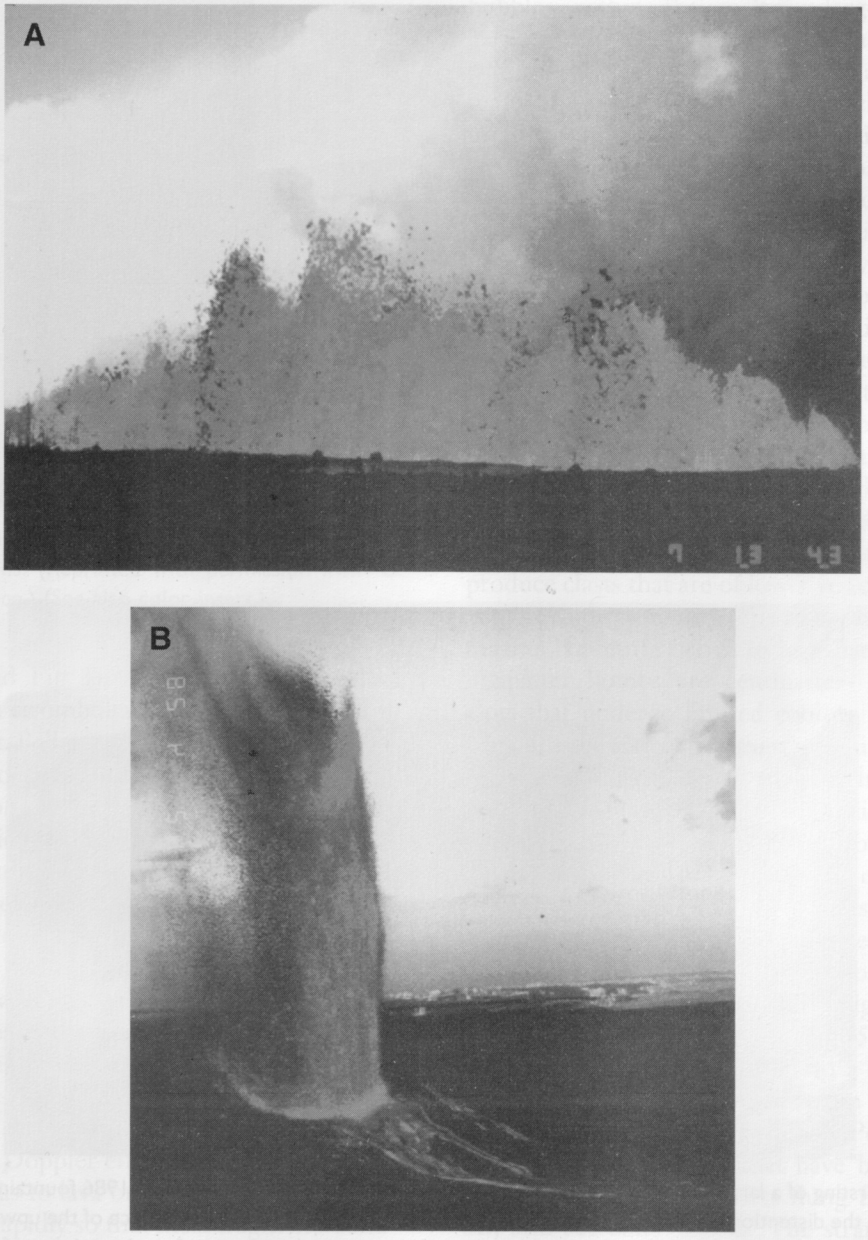

FIGURE 1 (A) A 60- to 100-m-high curtain of fire from the opening stages of the 1983 to present eruption of Kilauea volcano, Hawaii. The photograph shows a 500-m-long segment of an eruptive fissure that extended for 1 km. (Photograph by J. Griggs, U.S. Geological Survey.) (B) A 395-m-high lava fountain from the 1983–1986 fountaining episodes of Kilauea volcano, Hawaii. The photograph was taken 8 minutes before fountaining ceased. (Photograph by G. Ulrich, U.S. Geological Survey.)

cano at the Pu'u'O'o and adjacent Kupaianaha vents, which started in 1983 and continues at the time of this writing, is a prime example of the explosive to effusive transition common to basaltic eruptions. In this instance, the initial fissure opening was followed by 3 years of high lava fountains occurring on a predictable schedule of one fountaining episode every 25 days, on average. These spectacular events gave way in 1986 to near-continuous, low-level lava effusion, which persists after nearly 13 years of activity.

Strombolian eruptions start with a hawaiian-style fissure eruption, or, alternatively, a vent-clearing vulcanian explosion of rock and ash. The magma involved is often of higher viscosity, because of both cooler eruption tem-

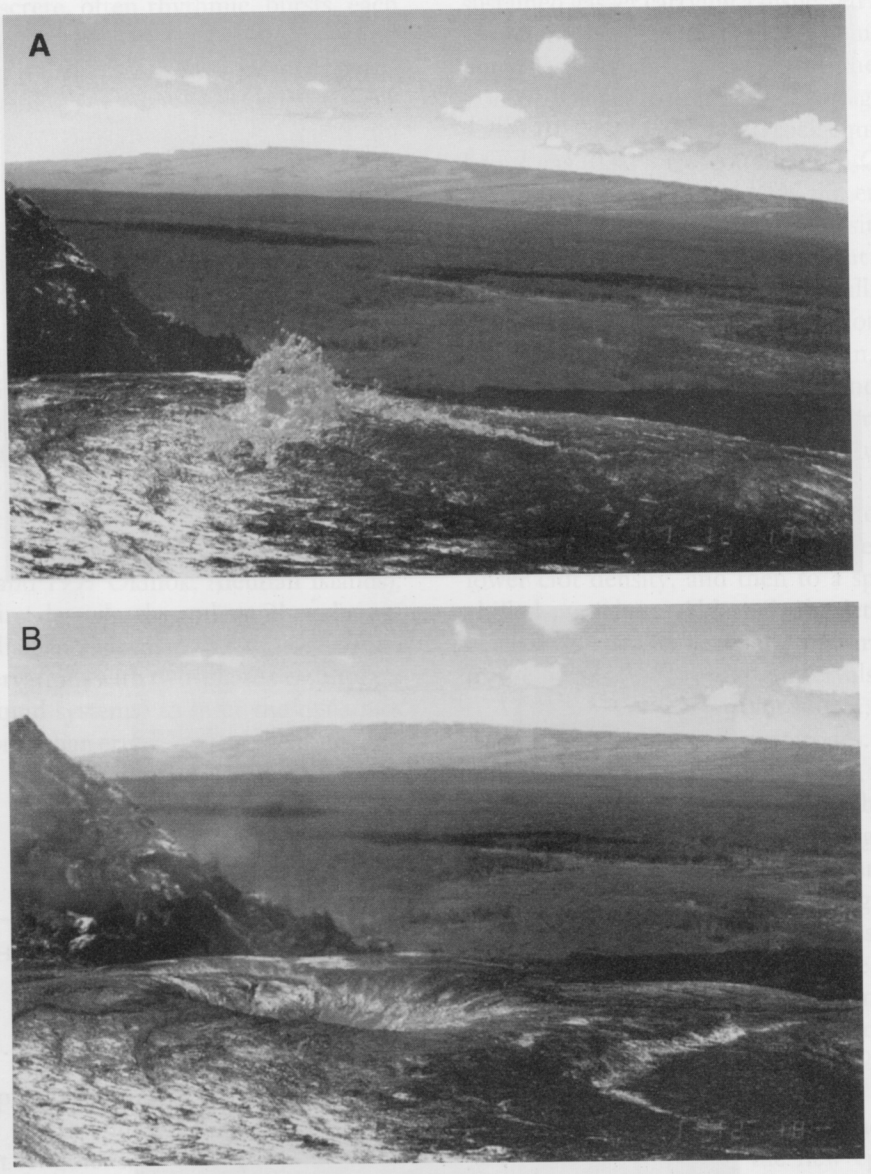

FIGURE 2 (A) Bursting of a large gas bubble in repose-period gas–pistoning during the 1983–1986 fountaining episodes at Kilauea volcano, Hawaii. Note the distention and tearing of the uplifted, pliable lava crust covering the surface of the upwelling lava. (Photograph by G. Ulrich, U.S. Geological Survey.) (B) Drainback of lava into the vent as seen 1 min after the release of the gas pocket in (A). (Photograph by G. Ulrich, U.S. Geological Survey.)

peratures (e.g., 1080°C is common at Mount Etna) and the involvement of slightly more siliceous magmas, typically in the basaltic andesite range. Gas release is episodic, leading to larger overpressures, more intense eruptions, and higher degrees of magma breaking (i.e., smaller ejecta sizes) relative to hawaiian-style activity. Prior to each explosion, gas accumulates in the conduit in a large bubble that rises and lifts the lid of overlying magma to form a gas-filled blister several meters in diameter. The blister swells and eventually explodes with a resounding roar, perhaps ≈1–10 s in duration, expelling a spray of gas loaded with centimeter- to meter-sized fragments of the disrupted lid (Fig. 3; see also color insert).

Overall, the flux of gas relative to lava in strombolian eruptions is considerably larger than in hawaiian erup-

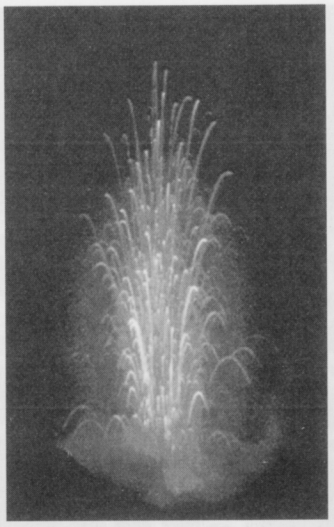

FIGURE 3 April 1992 strombolian explosion at Stromboli volcano, Aeolian Islands. (Reprinted with permission from G. Brandeis, O.M.P., France.) (See also color insert.)

tions (cf. Fig 1 and Fig 3), mainly because the lava column involved in strombolian activity is confined to the volcanic conduit. Ballistic analysis of ejecta and modeling of jet dynamics for eruptions at Stromboli, Etna, Paricutin, and Tolbachik volcanoes suggest typical gas:lava volume ratios of $\approx 10^5 : 1$, with lava volume between 10^{-3} and 10^2 m^3 per explosion (dense rock equivalent) and gas volume of 10^3 m^3 per explosion. Photoballistic analysis of ejecta trajectories at Stromboli (1971) and Heimaey (1973), show that fragments exit the vent at angles of 45° to over 75° from the horizontal at speeds of 40–100 m s^{-1}, reaching heights greater than 100 m. The tracking of the smallest particles on a series of photographs suggests that gas velocities are roughly double that of most magma fragments. Recent measurements based on the Doppler effect show similar results. The high ratio of gas to lava on ejection allows heat to dissipate relatively rapidly so that most fragments solidify in the air during flight.

Strombolian explosions characteristically occur at quasi-regular intervals. Ongoing activity at Stromboli volcano, for example, averages 3–5 explosions/hour. Violent but rare episodes at Stromboli exhibit cycles of 100 to 1000 explosions/hour.

B. Eruptive Products

During hawaiian fire fountains and strombolian explosions, magma fragments into bubbly, molten clots. Gas bubbles within the melt undergo decompressional expansion in the conduit and in the eruption column, causing the bubbly melt to expand as it rises (see Magmatic Fragmentation). The largest clots and those rising in the core of the fountain remain sufficiently fluid through transport and deposition to coalesce at the vent into rootless lava flows or lava ponds (Fig. 1B). Others cool rapidly as they mix with entrained air, or quench, and are deposited as discrete, glassy clasts. In many instances the deformation that the molten droplet has experienced in response to aerodynamic forces and surface tension is preserved in the clot by quenching. The timing of quenching, the magnitude and rate of decompression during magma ascent, and the temperature, composition, and viscosity of the melt control the crystallinity (volume percent crystals relative to glass) and vesicularity (volume percent gas bubbles relative to crystals plus glass) of the quenched clast. Strombolian eruptions often produce clasts that are of lower vesicularity and marginally higher crystallinity (due to cooling at the top of the magma column) relative to hawaiian eruptions.

Spatter bombs are centimeter- to decimeter-sized clots that undergo limited cooling prior to deposition (Fig. 4A; see also color insert). A thin skin of congealed lava forms on the exterior of the bomb during flight, but the clot as a whole remains sufficiently fluid to flatten upon landing and anneal, or weld, to an existing surface. Slow postdeposition cooling and degassing creates a finely crystalline interior interspersed with irregularly shaped relict gas bubbles, or vesicles.

Pele's tears are small droplets of shiny black glass molded and quenched during flight into spherical, dumbbell, or tadpole shapes (Fig. 5A). These droplets range from a few millimeters to a few centimeters in size and can be quite vesicular (up to 70%), although they are more commonly dense. Pele's hair are long, golden threads of glass that have been drawn out, or spun, from molten droplets flung from the vent (Fig. 5B; also see color insert). The strands are cylindrical, with diameters of 1–500 micrometers and can be up to 1 m in length. The thickest strands (>50 micrometers) contain stretched vesicles parallel to the long axis. These clasts are readily carried by wind and can be found tens of kilometers from the vent.

Scoria are thoroughly quenched, frothy clasts centimeters in size that are sufficiently porous and brittle to break when they hit the ground (Fig. 4A). Vesicularities between 70 and 85% and crystallinities of 2–50% are commonly observed (e.g., Kilauea, Etna, Mount Lassen, Paricutin, Izu-Oshima, Stromboli). Scoria with extremely high vesicularities of 95 to 99% are produced

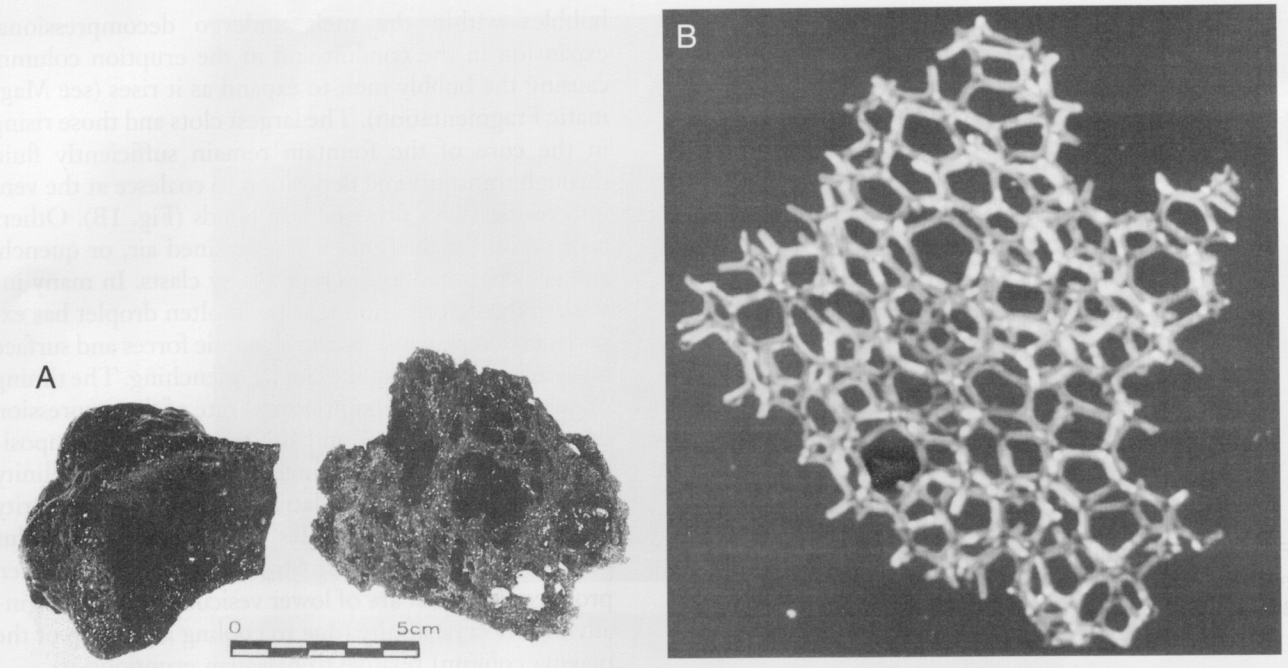

FIGURE 4 (A) Scoria (right) and spatter bomb (left) from the 1983–1986 fountaining events at Kilauea volcano, Hawaii. The frothy scoria clast has a vesicularity of 85% and a bulk density of 400 kg m^{-3}, and the spatter bomb 65% and 900 kg m^{-3}, respectively. (Photograph by J. Griggs, U.S. Geological Survey.) (B) Reticulite from a 1983–1986 fountaining episode at Kilauea volcano. The 1-cm clast has a vesicularity of 98%, and a bulk density of 50 kg m^{-3}. (Photograph by M. Mangan, U.S. Geological Survey.) (See also color inserts.)

in high lava fountains and have been quenched while expanding. These fragile clasts, known as reticulite, have the appearance of a delicate, golden-brown honeycomb (Fig. 4B) in which close packing has deformed bubbles into 12- to 14-sided polygons. Relict bubble walls, ≤ 1 μm thick, are mostly shattered, and virtually no closed space exists in the clast.

C. Deposition Features

The low eruption column and coarseness of the ejecta produced in hawaiian and strombolian eruptions limit their dispersal potential. More than half of the ejecta falls within approximately 500 m of the vent in spatter cones or cinder cones (see Scoria Cones and Tuff Rings). These conical deposits, which may reach heights of 100 m or more, are in stark contrast to the massive sheet-like deposits produced in more explosive types of volcanism (e.g., plinian).

Spatter cones form when partially molten clots fall to the base of a lava fountain and enclose the vent in a ring of welded clasts. Very fluid clots may become trapped and coalesce within the developing ring, creating a molten pond that gradually deepens as the ring grows taller and more cone-like. A cinder cone formed in strombolian eruptions, in contrast, is composed of loose, nonwelded clasts because most of the ejecta are rigid at the time of deposition. Rates of cone building in hawaiian and stromblian eruptions may exceed 5 m $hour^{-1}$.

Typically, a small volume ($<$1–20%) of millimeter- to centimeter-sized clasts (scoria, reticulite, Pele's tears, and hair) blanket areas surrounding the vent, especially on the downwind side (Fig. 1B). The sheet-like deposit thins abruptly outward from the spatter (or cinder) cone, generally diminishing to 10% of the maximum near-vent thickness over dispersal areas of <10 km^2 (e.g., Kilauea, Hawaii; Serra Gorda, Azores; Teneguia, Canary Islands, Heimaey, Iceland; Mount Etna, Sicily). In plinian deposits a 10% diminution in thickness in likely to occur over an area of >1000 km^2.

Of less importance in terms of ejecta dispersal and deposition is the dilute convective plume of volcanic gas, aerosols, and ash that forms above the eruption column during hawaiian and strombolian events. These plumes contain $<0.17\%$ of the total mass fraction of lava erupted and rarely penetrate the tropopause.

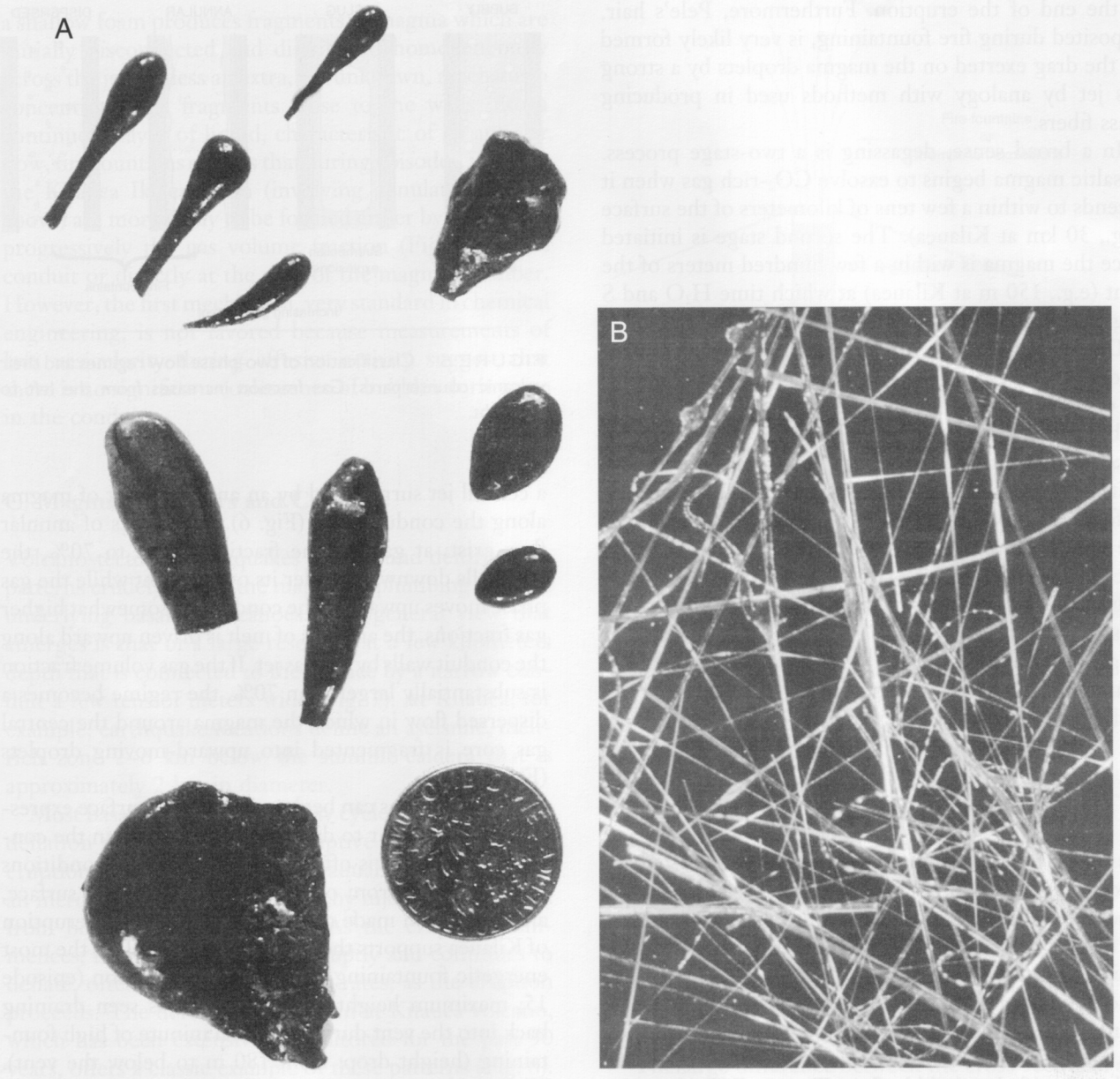

FIGURE 5 (A) Pele's tears: quenched droplets of lava shaped by surface tension and aerodynamic forces upon ejection from the vent. (Photograph by J. Griggs, U.S. Geological Survey). (B) Pele's hair: quenched filaments spun from molten droplets by turbulent air/gas mixing upon ejection from the vent. (Photograph by M. Mangan, U.S. Geological Survey.) (See also color insert.)

II. DYNAMIC PROCESSES

A. Degassing

Basaltic volcanoes display varied and complex behavior due to the existence of a separate and evolving gas phase. Gas emission measurements at Kilauea, Etna, Stromboli, and Pacaya have shown that hawaiian and strombolian eruptions involve the evolution and release of $\approx 10^5$ metric tons/day of H_2O-, CO_2-, and S-rich gas during peak activity. Further, evidence for the importance of the gas phase in eruption processes comes from the fragmentation of magma into discrete, highly vesiculated ejecta, the existence of a volcanic plume above the eruption column, and the deep draw-down of magma

at the end of the eruption. Furthermore, Pele's hair, deposited during fire fountaining, is very likely formed by the drag exerted on the magma droplets by a strong gas jet by analogy with methods used in producing glass fibers.

In a broad sense, degassing is a two-stage process. Basaltic magma begins to exsolve CO_2-rich gas when it ascends to within a few tens of kilometers of the surface (e.g., 30 km at Kilauea). The second stage is initiated once the magma is within a few hundred meters of the vent (e.g., 150 m at Kilauea) at which time H_2O and S begin to exsolve in significant amounts.

During both stages, volatile exsolution during ascent leads to the nucleation of bubbles and their growth both by chemical diffusion and decompressional expansion. Bubble growth is initially dominated by diffusion, with decompressional growth becoming increasingly important as the magma approaches the vent. There may be differential movement of melt and gas resulting from the size-dependent buoyancy of individual bubbles relative to the rise velocity of the magma. In general, the larger CO_2-rich bubbles generated at depth are likely to be sufficiently buoyant to rise up through the ascending magma whereas the smaller H_2O-rich bubbles generated near the surface are quasi-stationary in relation to the melt.

B. Two-Phase Flow

A useful way of examining the behavior of a melt-bubble mixture is provided by the separated two-phase flow models developed in chemical engineering applications. In this context, specific regimes are classified on the basis of gas volume fraction, which determines the geometry and partitioning of gas "elements" in the melt rising in the conduit. For a gas content of less than 30%, the melt contains small, discrete bubbles in suspension and is classified as bubbly flow (Fig. 6). Effusive eruptions are the consequence of bubbly flow in the conduit.

At gas contents of about 70%, small bubbles may coalesce, either in the magma reservoir or in the transport system, to produce large gas pockets that fill the entire width of the volcanic conduit (Fig. 6). These gas pockets are separated by smaller regions of bubbly magma and this regime is called slug flow. Strombolian explosions and the gas–piston events observed between some eruptive episodes are the surface expression of slug flow. Both phenomena are due to the bursting of a large slug of gas at the top of the magma column.

Slug flow makes a transition to annular flow at gas volume fractions above 70%. In this regime, gas forms

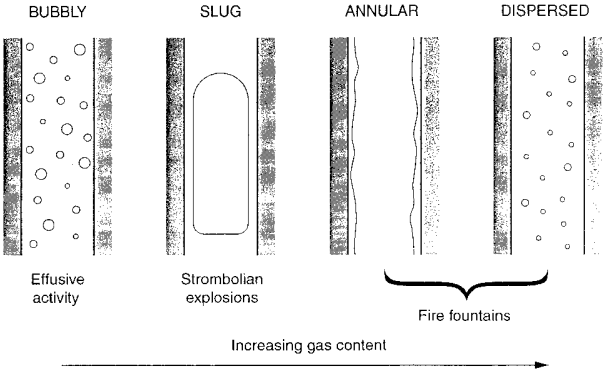

FIGURE 6 Classification of two-phase flow regimes and their volcanic counterparts. Gas fraction increases from the left to the right.

a central jet surrounded by an annular sheet of magma along the conduit walls (Fig. 6). Two types of annular flow exist: at gas volume fractions close to 70%, the melt falls downward under its own weight while the gas phase moves upward in the conduit. At somewhat higher gas fractions, the annulus of melt is driven upward along the conduit walls by the gas jet. If the gas volume fraction is substantially larger than 70%, the regime becomes a dispersed flow in which the magma around the central gas core is fragmented into upward-moving droplets (Fig. 6).

Lava fountains can be described as the surface expression of an annular to dispersed flow regime in the conduit. Although it is often difficult to deduce conditions in the conduit from observations made at the surface, an observation made during the 1959 summit eruption of Kilauea supports the annular flow model. In the most energetic fountaining episode of the eruption (episode 15; maximum height: 570 m), lava was seen draining back into the vent during the final minute of high fountaining (height drop: from 180 m to below the vent). The simultaneous motion of liquid upward in the fountain and downward in the conduit is suggestive of a transition between the two types of annular flow described above.

However, some numerical models suggest that a fire fountain corresponds to a dispersed flow. There are only two primary mechanisms by which a dispersed flow can be produced in the conduit: in the first process, the gas volume fraction is slowly increased from bubbly to slug and annular flows (Fig. 6), whereas in the second one the coalescence of a foam trapped in the shallowest part of the magma conduit causes fragmentation, a mechanism very similar to that involved in the formation of plinian eruption columns. However, the coalescence of

a shallow foam produces fragments of magma which are initially disconnected and distributed homogeneously across the jet. Unless an extra, yet unknown, mechanism concentrates the fragments close to the walls into a continuous layer of liquid, characteristic of an annular flow, fire fountains such as that during episode 15 during the Kilauea Iki eruption (involving annular flow, see above) are more likely to be formed either by increasing progressively the gas volume fraction (Fig. 6) in the conduit or directly at the roof of the magma chamber. However, the first mechanism, very standard in chemical engineering, is not favored because measurements of lava vesicularity during effusive activity suggest that there is no significant coalescence of bubbles during rise in the conduit.

C. Magma Reservoirs and Conduits

Volcano-tectonic earthquakes and ground deformation patterns crudely define the magmatic plumbing systems underlying basaltic volcanoes. The general view that emerges is that of a large reservoir at a few kilometers depth that is connected to the surface by a narrow conduit a few tens of meters wide (Fig. 7). At Kilauea, for example, earthquake locations define an aseismic, melt-rich zone 2–6 km below the summit caldera that is approximately 2 km in diameter.

Most basaltic volcanoes display cycles of inflation and deflation that correlate with eruptive events. Before an eruption, the ground surface gradually inflates due to an increase in reservoir pressure by injection of magma from below and/or degassing. As the eruption commences, the volcano deflates abruptly and continues to deflate, often at somewhat lower rates, as the eruption proceeds. The deformation pattern at Kilauea volcano, which has been extensively monitored for the past 30 years, offers a classic example of these patterns (Fig. 8). The center of deformation at Kilauea shifts within the summit region over time, suggesting that the reservoir may actually consist of several, smaller, interconnected chambers. Deformation and seismicity also show steeply dipping tabular bodies of magma along the volcano's two rift zones radiating outward to the southwest and to the east of the summit. A rift zone reservoir is located ≈2.5 km beneath the currently active Pu'u'O'o vent, for example, which is continuously fed magma from Kilauea's summit reservoir more than 15 km away. At the time of its emplacement it was estimated to be 2.5 km high, 11.0–15.0 km long, and 3.5 km wide. Similar deformation patterns have been observed on some strombolian volcanoes.

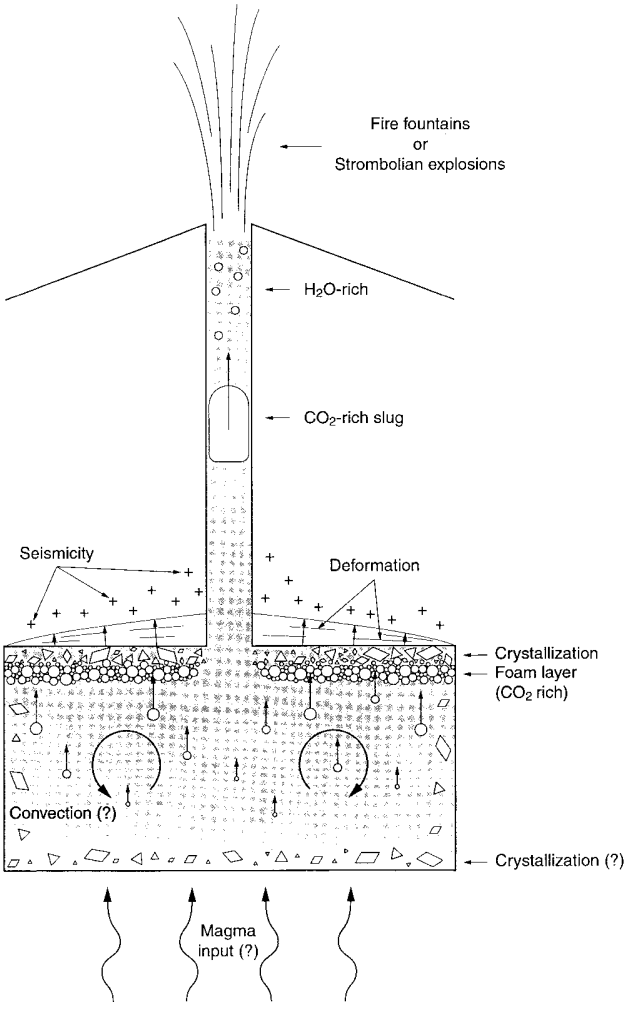

FIGURE 7 Sketch of a basalt volcano and phenomena related to magma storage and eruption.

The large difference between the cross-sectional area of the roof of the magma reservoir, which at Kilauea is ≈30 km^2, and that of the connecting conduit, which is likely to be ≤0.001 km^2, imposes a strong constraint on the velocity of magma ascent. Because mass flux must be conserved between the magma chamber and the vent, the drastic reduction in cross-sectional area requires a very large increase in velocity. For example, a small upward velocity of 10^{-5} m s^{-1} in the magma chamber produces a velocity of 1 m s^{-1} at the vent. In addition, the large difference in density between a slightly bubbly liquid and a gassy lava fountain can lead to a 100-fold increase in the velocity between the bottom and the top of the volcanic conduit.

Eruptions may be triggered by crystallization and ve-

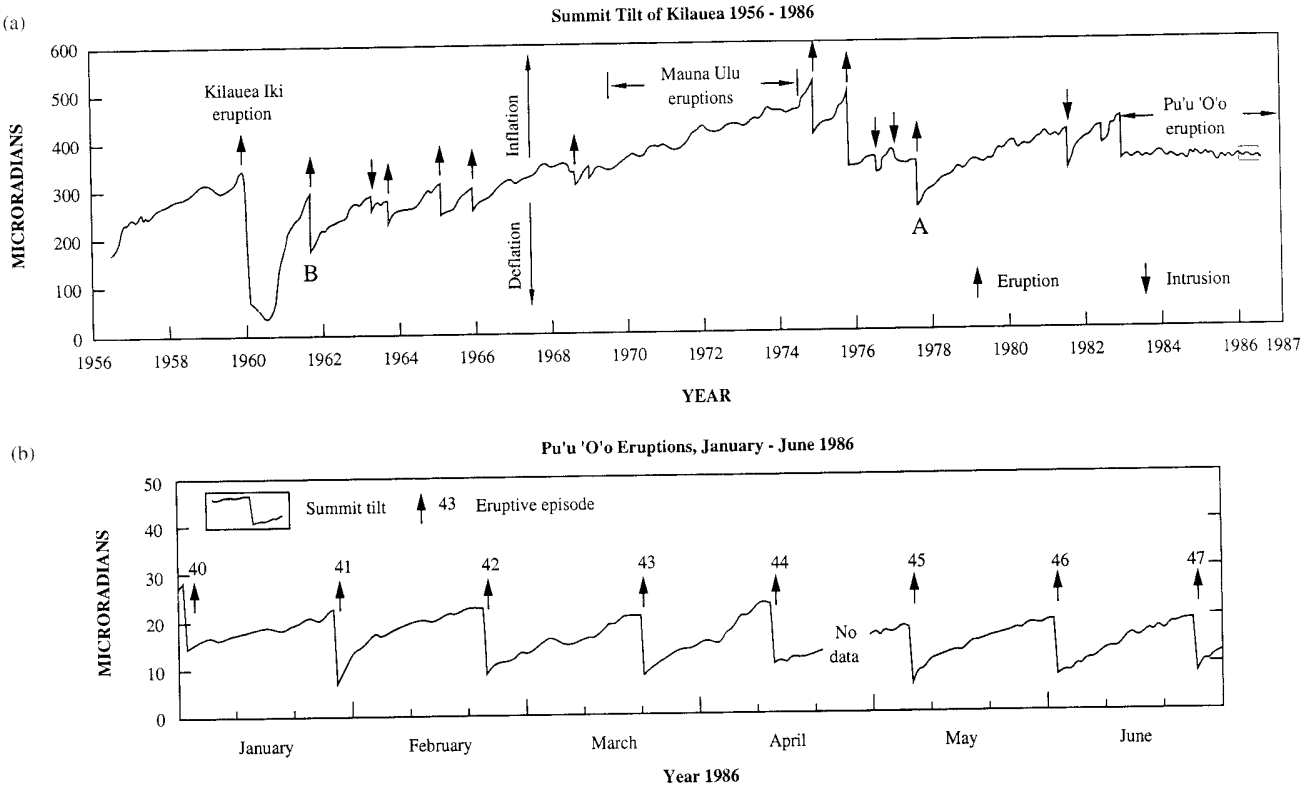

FIGURE 8 Summit tilt deformation (East–West component) at Kilauea volcano, Hawaii (from Tilling *et al.*, 1987; see text): (a) for the past 30 years; (b) during fire fountains.

siculation in the magma chamber. Cooling of reservoirs leads to the formation of crystals, thus enriching the remaining melt in volatiles. When the solubility limit is reached, gas exsolution occurs and the magma chamber increases in both volume and pressure as vesiculation proceeds. Ultimately, the internal pressure may exceed the strength of the surrounding rocks to trigger an eruption. Alternatively, replenishment from a deep magma source may be the triggering mechanism. The input of an additional volume of a bubbly magma combined with the volume increase due to decompressional expansion of tiny bubbles that enter and rise toward the roof of the chamber, may sufficiently pressurize the system to trigger an eruption. The presence of gas bubbles in basaltic magma chambers also has consequences for the development and duration of an eruption as shown at Kilauea Iki (Hawaii), where bubble diameters in the reservoir are ≈0.4 mm.

D. Sources of Vibration

Other constraints on the dynamics of transport emerge from the analysis of volcanic tremor, which is a continuous vibration of the ground around active volcanoes. Volcanic tremor is usually characterized by a sharply peaked spectrum with one dominant and several subdominant peaks (Figs. 9, 10a, and 10b). The tremor recorded during lava fountain episodes at Kilauea has several peaks between 3 and 10 Hz (Fig. 9) and is produced at a depth of <1 km. Tremor recorded during the repose periods, as well as during gas-piston events, shows only two dominant peaks between 2 and 4 Hz. Resonators of various geometries have been called upon to explain volcanic tremor, from the vibration of a crack filled by liquid, to the vibration of a spherical magma chamber. The role of gas as a trigger was suggested at Kilauea because of the similarity between tremor and the seismicity induced by gas–piston events. Gas–pistoning generates a unique signature consisting of a spindle-shape amplitude envelope persisting for a duration of 80 s. Visual observations confirm that each "spindle" correlates with the bursting of large gas bubbles at the top of the magma column.

At Stromboli, the main peak in the tremor is approximately 2 Hz with a secondary peak slightly above 4 Hz. The depth at which the tremor is produced is, for the most part, less than 200 m and results from continuous

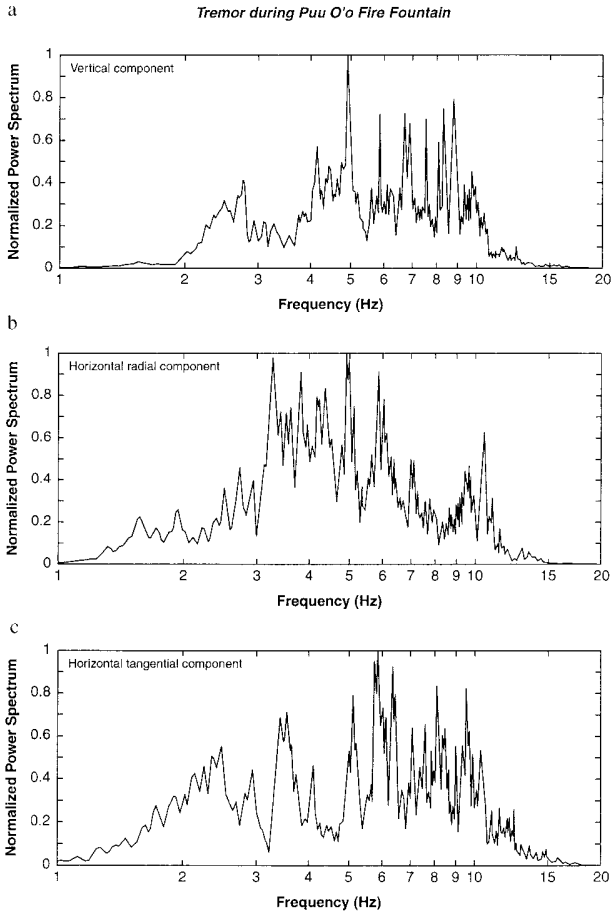

FIGURE 9 Tremor recorded during the Pu'u 'O'o fire fountain, Hawaii (from Koyanagi *et al.*, 1987; see text): (a) vertical component; (b) horizontal radial component; (c) horizontal tangential component.

bursting of small gas bubbles. However, its frequency of ≈2 Hz can also be interpreted as oscillations of a bubble cloud 50 m in length, with 1% gas volume fraction. Both are reasonable values for the height of the shallow magma column and the gas content at Stromboli. With the development of broad band seismometers, more is to be learned in the future from tremor at periods less than 1 s because it offers constraints on pressure fluctuations resulting from unsteady magma transport.

The pressure waves induced by explosions have been measured at Stromboli volcano and provide additional constraints on conduit transport (acoustic measurements). Although the audible sound radiated by an explosion is very striking, most of the acoustic energy is infrasonic, i.e., below 20 Hz (Fig. 10c). The power spectrum of acoustic pressure before an explosion is very similar to the seismic recording (Fig. 10b and 10c) with a powerful peak at ≈2 Hz. However, during explosions the acoustic frequency shifts toward a higher frequency of ≈10 Hz. The strong acoustic pressure recorded during explosions (Fig. 11) has been associated with the breaking of a gas bubble with a radius of a few meters that is still overpressurized (by 0.3 10^5 Pa) at the top of the magma column. Because the vibration of the bubble in air does not have direct interactions with the solid walls of the conduit (part 2; Fig. 11) no seismic waves at ≈10 Hz are produced in the volcanic edifice (Fig. 10b). Sound waves, albeit of very low intensity, can also be generated by oscillations of the magma column induced by a rising bubble (Fig. 11, part 1), or by oscillations of the bubble bottom after the gas pocket breaks

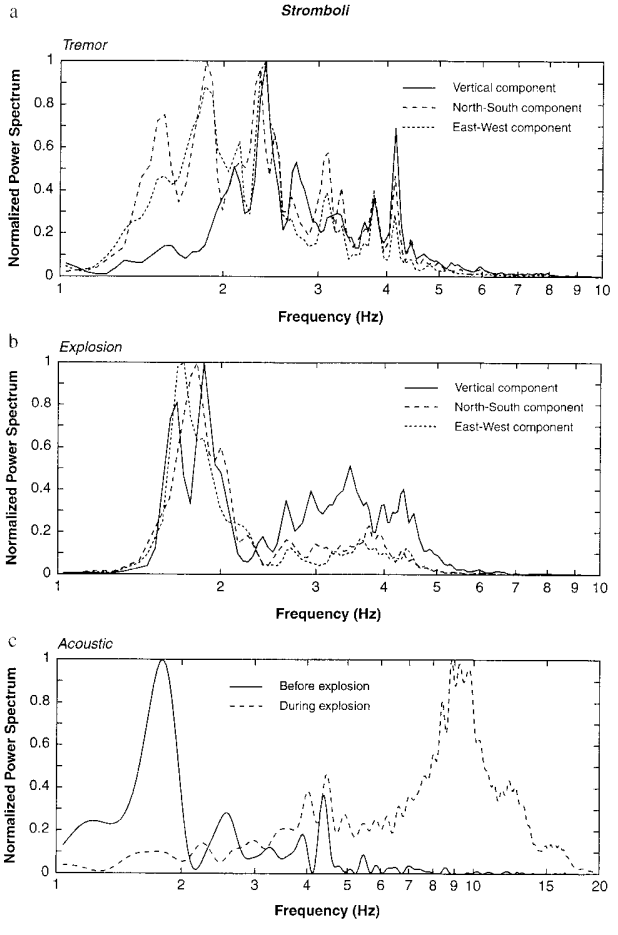

FIGURE 10 Stromboli. (a) Seismicity during tremor (reprinted with permission from Chouet *et al.*, 1997); (b) seismicity during an explosion (reprinted used with permission from Chouet *et al.*, 1997); and (c) acoustic pressure before and during an explosion (reprinted with permission from Vergniolle *et al.*, 1996). Note the similarity in power spectra.

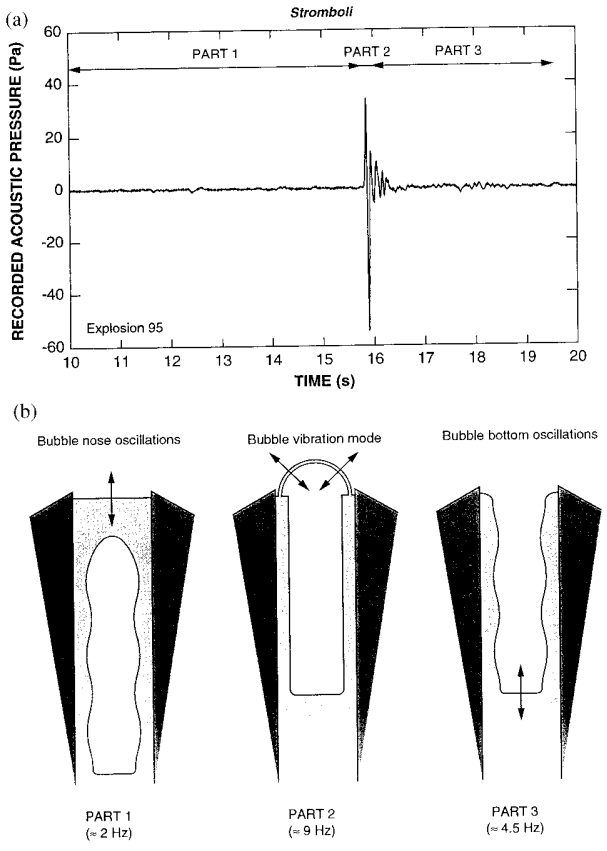

FIGURE 11 (a) Measurements of acoustic pressure at Stromboli. (b) Sketch of the three stages of bubble rise corresponding to the three parts in acoustic pressure. (Reprinted with permission from Vergniolle *et al.*, 1996).

(Fig. 11 part 3). By combining these oscillations, the magma viscosity is estimated at ≈300 Pa s. In very quiet conditions, bubble rise can be followed on acoustic records (the ≈2-Hz mode) in the uppermost 30 m of the magma column. An alternate explanation for the sound waves at Stromboli is that the acoustic sources of the explosions lie at depth and the resonant modes of a magma column can be calculated from them.

III. ERUPTION MODELS

The evolution and release of a separate gas phase induces complex, time-dependent behavior, and two general approaches have been taken to examine and explain these complexities. Both models recognize that variations in eruptive behavior are the consequence of the volume of gas present and how this volume is partitioned in the melt: small gas volumes lead to effusive eruptions and lava flows (bubbly flow), whereas large gas volumes cause either strombolian explosions as large gas pockets reach the surface (slug flow) or continuous gas jetting as in hawaiian lava fountains (annular or dispersed flow). The models differ in how and where gas separates from the melt.

The first of the two models uses numerical methods to investigate the rise and expansion of an initially bubbly mixture in the conduit. The decompression of a bubbly magma during rise leads to nucleation and growth of new gas bubbles as well as continued growth of the original bubbles. The model suggests that it is the extent of bubble coalescence (mechanism by which numerous small bubbles are transformed into a smaller number of larger bubbles) that occurs in the conduit during magma ascent that distinguishes hawaiian from strombolian eruptions. Coalescence, in turn, is controlled by the ascent rate of the magma. Slow magma rise may facilitate coalescence because transit times are long and bubbles have ample opportunity to overtake, collide, and coalesce with one another. An initially homogeneous population of small gas bubbles rising in the conduit could thus form large gas slugs that rise through the melt column and burst at the surface in classic stombolian style.

Higher magma rise rates may limit coalescence because the distance bubbles travel relative to the melt is small and the transit time is short, making bubble collisions less likely. The mixture remains essentially homogeneous until the volume fraction of exsolved gas reaches a critical point where bubbles become so closely packed that they deform and burst (≈75% by volume), causing the magma to fragment. Subsequent rise of the disrupted mixture of gas and clots (dispersed flow) leads to considerable expansion in the conduit, resulting in the formation of lava fountains. The flow conditions in the fountain, such as the emitted mass flux and the exit velocity and pressure, are strongly dependent on the geometry of the conduit and vent. The episodic fountaining pattern exhibited by many hawaiian eruptions is modeled by nonuniform magma cooling that creates a temporary "plug" at narrow sections of the plumbing system of sufficient yield strength to stop the flow of magma between two successive fire fountains.

In the 1990s, two-phase flow concepts and laboratory experiments have been combined and they offer an alternative view. In this model variations in eruptive style are the consequences of the differential motion of bubbles compared to magma inside a large magma reservoir (Fig. 7). A laboratory volcano has been built with a large reservoir filled with viscous oils topped by a narrow conduit. During the experiment, small gas bubbles

formed at the bottom of the chamber rise and accumulate in a foam layer at the roof of the chamber (Figs. 12 and 13). Bubbles in the foam deform as the layer builds and eventually collapse on masse. Sudden coalescence of bubbles in the layer creates a large gas pocket that rises in the conduit and bursts at the surface. Foam accumulation then resumes and a new cycle begins.

This pattern of foam buildup and coalescence is very regular for a given melt viscosity, which dictates the volume of gas in the gas pocket and the timing between the creation and ascent of successive gas pockets. Hawaiian-style lava fountains were qualitatively reproduced using a liquid of relatively low viscosity (0.1 Pa s). These experiments generated a foam layer that gave rise to a large, single gas pocket upon collapse. The ensuing "eruption" is that of a central gas vent surrounded by a film of liquid along the walls of the conduit (annular flow; Fig. 12). Minor and frequent coalescence events occurred at the top of the reservoir between successive total collapses, the former being reminiscent of the gas–piston activity often observed between fountaining episodes in hawaiian eruptions. Strombolian activity is reproduced by experiments using more viscous oils (1 Pa s). Here, collapse involves only parts of the foam and a number of intermediate size gas pockets are produced. The pockets rise and burst intermittently at the top of the conduit (slug flow; Fig. 13). This regime corresponds to a quasi-stagnant liquid column (Fig. 13), analogous to most strombolian eruptions in contrast to the previous regime (Fig. 12) in which huge variations in liquid levels exist, similar to the difference in height between a fire fountain and effusive activity.

In all experiments a critical gas flux to the roof is required for the foam to thicken and ultimately collapse.

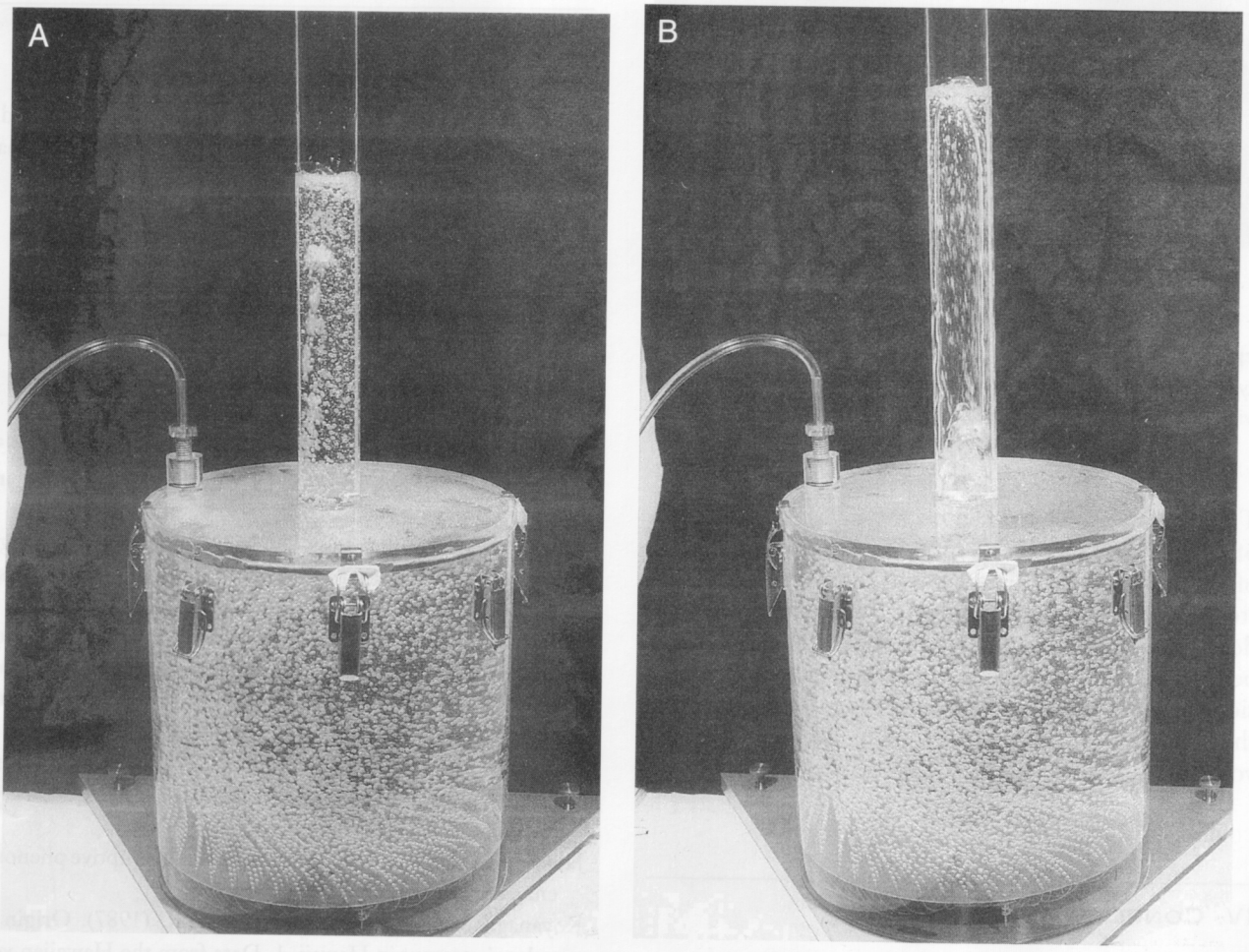

FIGURE 12 Laboratory volcano model using the low viscosity oil (0.1 Pa s), analogous to a hawaiian eruption. (Reprinted with permission from Vergniolle and Jaupart, 1990.) (A) Buildup of the foam at the top of the reservoir. Regime analogous to effusive activity. (B) Foam collapse and gas pocket rise in the conduit. Regime is analogous to fire fountain.

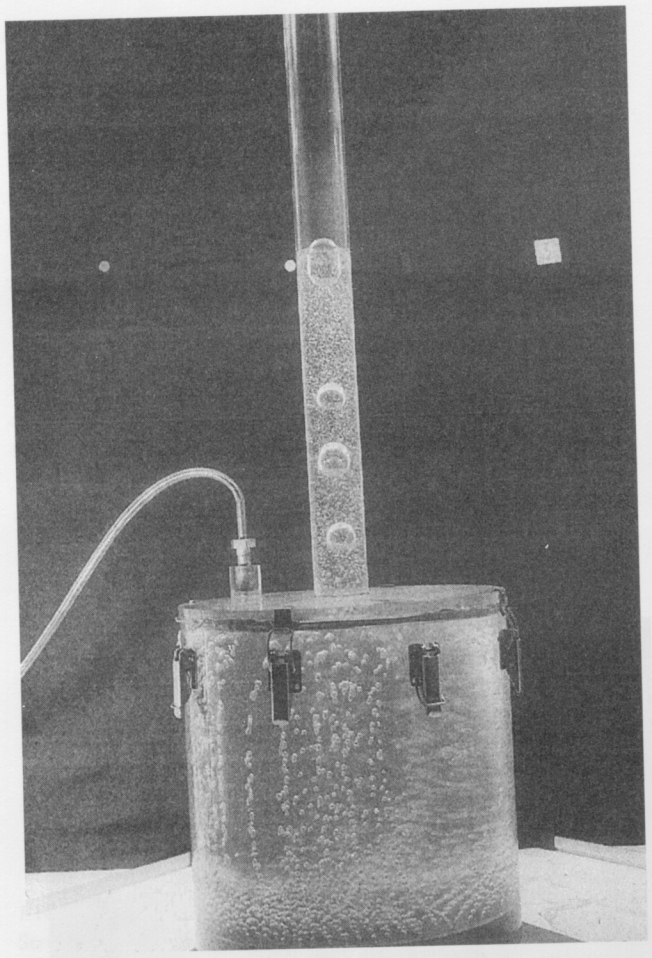

FIGURE 13 Laboratory volcano with a more viscous viscosity oil (1 Pa s), analogous to a strombolian eruption. (Reprinted with permission from Vergniolle and Jaupart, 1990.)

The threshold is dependent on the size and proportion of rising bubbles and the viscosity and surface tension of the melt. At less than critical gas fluxes there is a steady stream of foam rising in the conduit (bubbly flow), and the "eruption" is effusive. The transition between cyclic fountaining episodes to quiescent effusion that is often observed in hawaiian eruptions may thus be a reflection of a waning gas flux to the reservoir roof.

IV. CONCLUSION

Although more quantitative field measurements of variables such as pressure, velocity, and gas content will be useful for constraining models more tightly, a general pattern for basaltic eruptions is starting to emerge, showing, in particular, the importance of the role of the gas phase. Bubbles trigger eruptions and explain many of the features of hawaiian and strombolian eruptions. Lava flows are the consequence of the effusion at the vent of a bubbly flow in the conduit, whereas the most dramatic events in basaltic eruptions are related to very large gas pockets breaking at the vent and ejecting fragments of magma. Furthermore, there are rare situations in which basalts can erupt explosively in plinian basaltic eruptions, typical of a dispersed flow (Fig. 6). The continuum existing between hawaiian and strombolian activity is a direct consequence of the patterns of two-phase flow and the entire spectrum of flow regimes exist in basaltic eruptions.

SEE ALSO THE FOLLOWING ARTICLES

Basaltic Volcanoes and Volcanic Systems • Lava Flows and Flow Fields • Lava Fountains and Their Products • Magma Chambers • Plinian and Subplinian Eruptions • Rates of Magma Ascent • Scoria Cones and Tuff Rings

FURTHER READING

Chester, D. K., Duncan, A., Guest, J., and Kilburn, C. (1985). "Mount Etna, The Anatomy of a Volcano." Chapman and Hall, London.

Chouet, B. (1996). Pages 23–97 *in* "Monitoring and Mitigation of Volcano Hazards" (R. Scarpa and R. Tilling, Eds.). Springer-Verlag, Berlin.

Chouet, B., Saccarotti, G., Martini, M., Dawson, P., De Luca, G., Milana, G., and Scarpa, R. (1997). Source and path effects in the wave fields of tremor and explosions at Stromboli volcano. *J. Geophys. Res.* **102,** 15129–15150.

Gerlach, T. M. (1991). Exsolution of H_2O, CO_2 and S during eruptive episodes at Kilauea volcano, Hawaii. *J. Geophys. Res.* **91,** 12177–12185.

Jaupart, C., and Tait, S. (1990). Dynamics of eruptive phenomena. Rev. Miner. **24,** 213–238.

Koyanagi, R. Y., Chouet, B., and Aki, K. (1987). Origin of volcanic tremor in Hawaii. 1. Data from the Hawaiian volcano observatory 1969–1985. *U.S. Geol. Surv. Prof. Paper* **1350,** 1221–1257.

Mangan, M. T., and Cashman, K. V. (1996). The structure of basaltic scoria and reticulite and inferences for vesiculation, foam formation, and fragmentation in lava fountains. *J. Volcanol. Geotherm. Res.* **73,** 1–18.

Parfitt, E. A., and Wilson, L. (1995). Explosive volcanic eruptions-IX. The transition between Hawaiian-style lava fountaining and Strombolian explosive activity. *Geophys. J. Int.* **121,** 226–232.

Swanson, D. A., Duffield, D. A., Jackson, D. B., and Peterson, D. W. (1979). Chronological narrative of the 1969–1971 Mauna Ulu eruption of Kilauea volcano, Hawaii. *U.S. Geol. Surv. Prof. Paper* **1056,** 1–55.

Tilling, R. I., Heliker, C., and Wright, T. L. (1987). "Eruptions of Hawaiian Volcanoes: Past, Present, Future." Department of the Interior/U.S. Geological Survey.

Tilling, R. I., and Dvorak, J. (1993). Anatomy of a basaltic volcano. *Nature* **363,** 125–133.

Vergniolle, S., and Jaupart, C. (1990). The dynamics of degassing at Kilauea volcano, Hawaii. *J. Geophys. Res.* **95**(B3), 2793–2809.

Vergniolle, S., Brandeis, G., and Mareschal J-C. (1996). Strombolian explosions: Eruption dynamics determined from acoustic measurements. *J. Geophys. Res.* **101**(B9), 20449–20466.

Wallis, G. B. (1969). "One Dimensional Two-Phase Flows." McGraw-Hill, New York.

Wolfe, E. W., Garcia, M. O., Jackson, D. B., Koyanagi, R. Y., Neal, C. A., and Okamura, A. T. (1987). The Pu'u'O'o eruption of Kilauea volcano, episodes 1–20, January 3, 1983 to June 8, 1984, U.S. Geol. Surv. Prof. Paper **1350,** 471–508.